Chapter 3

On the Stability of Random Access with Energy Harvesting and Collision Resolution

Energy harvesting and finiteness of energy have gained a lot of interest recently. Several works have considered the losses in connectivity periods due to the limited available energy. Despite the advancement in energy harvesting and rechargeable batteries, the study of networks with energy harvesting nodes is still in its infancy. The common objectives were usually to maximize the lifetime of the network whose nodes are powered by rechargeable batteries, while maintaining a certain degree of connectivity [39].

Leveraging the feedback information can provide a degree of coordination between the nodes of a random access network[16]. This can result in a lower number of collisions, and hence, a reduction in energy consumption. Feedback information was exploited in several works related to cognitive radio networks. Secondary users are allowed to overhear the automatic repeat request (ARQ) [15] sent from primary receiver to primary transmitter, and take channel access decisions based on the overheard feedback, as introduced in [14].

This chapter focuses on the effect of finite energy sources and energy harvesting on the stability of a random access network. We consider a network with two nodes. Each having a queue to store packets, and a battery to store energy. The process of energy consumption from the battery during transmission, and its replenishment through energy harvesting is modeled by considering the battery as a queue with arrival and service rates determined by the energy harvesting and consumption rates, respectively. When a node has packets in its packet queue, it will attempt to transmit the packet at the head of the queue with some access probability if there is enough energy in its battery queue. If the transmission is successful, the packet is dropped from the queue. In case of a collision, the destination stores the collided packets, and sends negative acknowledgement (NACK). Making use of the NACK message, one node refrains from any transmission attempts, while the other node retransmits the collided packet. The destination can then use the retransmitted packet and the stored collided packets to recover the two packets involved in the collision. Therefore, the two nodes are served in two transmission attempts, but the retransmitting node has used more energy in the process.

In a random access network, the stability analysis usually involves interacting queues. For the slotted ALOHA protocol, the stability region is characterized for the case of $M = 2$ and $M = 3$ interacting queues as well as the case of $M > 3$ with symmetric arrivals. The stability region for the general case of $M > 3$ with asymmetric arrivals is still an open problem and only inner achievable bounds are known. Recently, many papers have considered the problem of interacting queues in different contexts. For example, [42] considers the problem

of interacting queues in a TDMA system where a relay is used to help the source nodes in forwarding their lost packets. In [43], the stability of interacting queues under a random access protocol in the context of *Cognitive Radio Network* was derived. In [44], the stability region of two interacting queues under random access protocol where the two queues harvest energy was characterized. Other works can be found in [45, 46], where derivations of the stability regions in the context of different cognitive radio networks were considered.

3.1 System Model

Fig. 3.1 depicts the model of the system under consideration. The system is comprised of two nodes transmitting to a common receiver in a random access fashion. Each node has an infinite queue, Q_i, $i = 1, 2$, to store fixed length packets. The arrival processes at the two queues are modeled as Bernoulli arrival processes with means λ_1 and λ_2, respectively [44]. Under our system model assumptions, the average arrival rates are λ_1 and λ_2 packets per time slot, and are bounded as $0 \leq \lambda_i \leq 1$, $i = 1, 2$[1]. We can assume that packets arrive at the start of the time slots.

To store energy, each node has a battery, also modeled as two queues, B_1 and B_2. Energy is assumed to be harvested in a certain unit and one unit of energy is consumed in each transmission attempt. The energy harvesting processes are modeled as Bernoulli arrival processes with means δ_1 and δ_2, respectively. Under our system model assumptions, the average energy arrival rates are δ_1 and δ_2 energy units per time slot[2], and are bounded as $0 \leq \delta_i \leq 1$, $i = 1, 2$ [44].

In this system, we consider a node to be active if both its packet queue and battery are nonempty at the same time, and idle otherwise. The channel is slotted in time and a slot duration equals one packet transmission time. The channel is modeled as a collision channel, where packet loss results only in the case of simultaneous transmissions from the two nodes. If only one node attempts transmitting at a given time slot, the packet is considered to be correctly received [44, 48]. If a node is active in a given time slot, it will attempt to access the channel with probability p_i, $i = 1, 2$.

[1]The maximum service rate in our model is 1 packet/slot, since the slot duration equals one packet transmission time, then the arrival rates must be less than 1 otherwise the system will be unstable.

[2]one energy unit is the energy needed to transmit one packet in one time slot

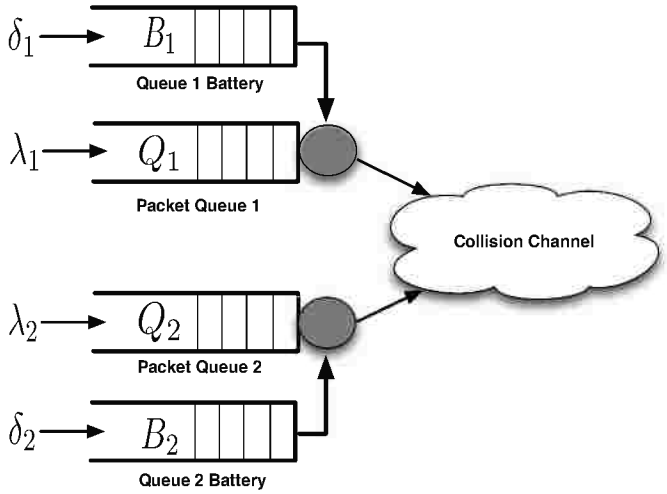

FIGURE 3.1: System model

In the case of a collision, nodes in our system leverage the feedback information received from the destination. When the two nodes attempt to transmit their packets simultaneously, the two packets collide, and the destination is unable to decode any of them. The destination stores the collided packets and sends negative acknowledgement (NACK). Upon receiving the NACK message, node 2 (Q_2) will back off and node 1 (Q_1) will retransmit its collided packet. The destination then uses the retransmitted packet and the stored collided packets to recover the two collided packets. Therefore, the two nodes are served in two time slots, but the retransmitting node consumes more energy than the backing off node.

3.2 The Stability Region for the Feedback-Based Random Access without Energy Harvesting

To set the benchmark, we will start by characterizing the stability region for the feedback-based random access scheme without energy constraints.

Stability can be loosely defined as having a certain quantity of interest bounded. In our case, we are interested in the queue size being bounded. For an irreducible and aperiodic Markov chain with countable number of states, the chain is stable if and only if it is positive recurrent, which implies the existence of its stationary distribution. For a rigorous definition of stability under more general scenarios see [48] and [49].

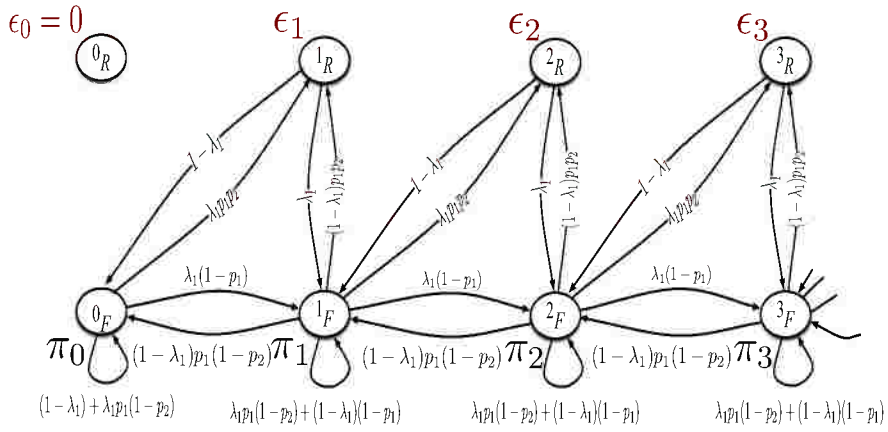

FIGURE 3.2: Queue 1, Q_1, Markov chain model for Dominant System 1.

If the arrival and service processes of a queueing system are strictly stationary, then one can apply Loyne's theorem to check for stability conditions [52]. This theorem states that if the arrival process and the service process of a queueing system are strictly stationary, and the average arrival rate is less than the average service rate, then the queue is stable, otherwise it is unstable.

In our system, and due to random access and possible collisions, the service rate of one node's packets queue depends on the state of the other node's packets queue (as well as the state of the batteries in both nodes, in the case of energy constraints). This results in an interacting system of queues, and complicates the stability region characterization. To decouple the queues interaction, we resort to the *Dominant System* concept proposed in [48] to characterize the stability region of the slotted ALOHA random access scheme. We will define two dominant systems tailored to match our feedback-based random access scheme. In each of the two systems we will determine the boundaries of the stability region. Finally, the stability region of our system is obtained as the union of the two dominant systems stability regions.

In a dominant system, we define a system that "stochastically dominates" our system, that is the queues lengths in the dominant system are always larger than the queues lengths in our system if both, the dominant system and our system, start from the same initial state and have the same arrivals and encounter the same packet collisions.

3.2.1 Dominant System 1

In this dominant system, we assume that Q_2 always have packets to transmit; even if the queue is empty, dummy packets are transmitted from Q_2. Clearly this will set a dominant system to our system since the transmission of dummy packets can only result in more collisions and packet losses. If for a given arrival rate pair (λ_1, λ_2) this dominant system is stable then clearly our system will be stable. Therefore, the stability region of this dominant system will provide an inner bound for our system's stability region.

Under this dominant system assumptions, the Markov chain describing the evolution of Q_1 is shown in Fig. 3.2. The Markov chain has two classes of states, namely, k_F and k_R and $k = 0, 1, 2, \cdots$. The subscript F denotes first transmission states and the subscript R denotes retransmission states. In the retransmission states, Q_1 packet will always be delivered since there is no collisions in these states (Q_2 is backing off). Q_2 packet is recovered from the retransmitted packet of Q_1 and the collided packets from previous state. In these retransmission states, either Q_1 length decreases by 1 if no arrival occurs to the queue or the length will remain constant if an arrival occurs since the packet on the head of the queue is successfully transmitted with probability 1.

The stability condition for Q_1 is given in the following lemma, which is proved in Appendix A.1.

Lemma 3.1. *For the system to be stable, the arrival rates for Q_1 and Q_2 in Dominant System 1 must satisfy the following two conditions.*

$$\lambda_1 < \frac{p_1}{1 + p_1 p_2}, \quad \lambda_2 < \frac{p_2(1 - \lambda_1 p_2 + \lambda_1^2 p_2 - \lambda_1)}{(1 - \lambda_1)}. \tag{3.1}$$

3.2.2 Dominant System 2

In this dominant system, we assume that Q_1 always has packets (dummy packets are sent if the queue is empty).

By the same argument used with dominant system 1, we can find the stability condition for dominant system 2 in the following lemma.

Lemma 3.2. *For the system to be stable, the arrival rates for Q_1 and Q_2 in Dominant System 2 must satisfy the following two conditions.*

$$\lambda_1 < \frac{p_1(1-\lambda_2 p_1+\lambda_2^2 p_1-\lambda_2)}{(1-\lambda_2)}, \quad \lambda_2 < \frac{p_2}{1+p_1 p_2}. \tag{3.2}$$

3.2.3 Overall Stability Region

The following Lemma characterizes the stability region for fixed random access probabilities, p_1 and p_2, for Q_1 and Q_2, respectively.

Lemma 3.3. *For a fixed random access probability vector $\mathbf{p} = [p_1\ p_2]^T$, the stability region $\mathcal{R}(\mathbf{p})$ of the feedback-based random access without energy constraints is the union of the two regions obtained from dominant systems 1 and 2, and is described by*

$$\lambda_2 < \frac{p_2(1-\lambda_1 p_2+\lambda_1^2 p_2-\lambda_1)}{(1-\lambda_1)} \text{ when } \lambda_1 < \frac{p_1}{1+p_1 p_2} \tag{3.3}$$

and

$$\lambda_1 < \frac{p_1(1-\lambda_2 p_1+\lambda_2^2 p_1-\lambda_2)}{(1-\lambda_2)} \text{ when } \lambda_2 < \frac{p_2}{1+p_1 p_2} \tag{3.4}$$

Proof. Here we provide a sketch of the proof due to space limitations. The result in Lemma 3.3 can be proved using the tool of stochastic dominance presented in [48]. The indistinguishability argument at the stability region boundary states that if the original system is unstable then its queues will saturate and they will always have packets to transmit; therefore at the boundaries of the stability region of the original system, the original system will be indistinguishable from the dominant system and thus has the same stability region boundaries [48]. □

The next theorem characterizes the entire stability region.

Theorem 3.4. *The boundary of the stability region, $\mathcal{R}$, of the feedback-based random access without energy constraints, is defined as the union*

$$\mathcal{R} = \bigcup_{\mathbf{p}\in[0,1]^2} \mathcal{R}(\mathbf{p}). \tag{3.5}$$

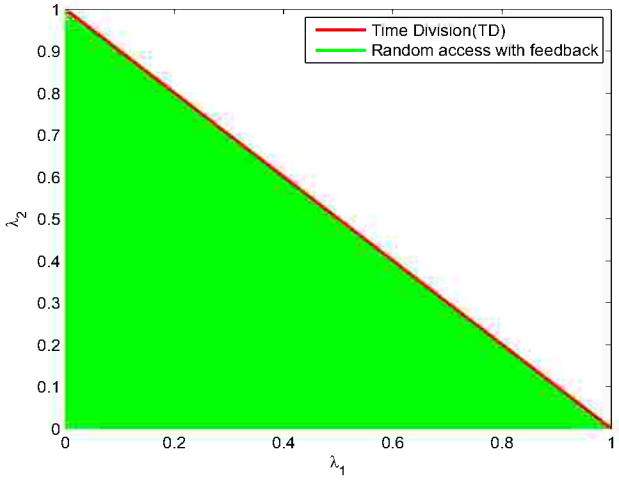

FIGURE 3.3: The stability regions for Random Access with Feedback, and Time Division schemes.

This union can be characterized as $\lambda_1 + \lambda_2 = 1$.

Proof. Here we provide a sketch of the proof due to space limitations. It can be easily proved that the stability region boundary given by $\lambda_1 + \lambda_2 = 1$ is spanned by the points $\left(\lambda_1 = \frac{p_1}{1+p_1p_2}, \lambda_2 = \frac{p_2}{1+p_1p_2}\right)$, with $p_1 = 1$ and $0 \leq p_2 \leq 1$ for $0 \leq \lambda_2 \leq \frac{1}{2}$ and with $p_2 = 1$ and $0 \leq p_1 \leq 1$ for $\frac{1}{2} \leq \lambda_2 \leq 1$. These access probabilities will achieve the $\lambda_1 + \lambda_2 = 1$ upper bound since if $p_1 = 1$ or $p_2 = 1$, then $\frac{p_1}{1+p_1p_2} + \frac{p_2}{1+p_1p_2} = 1$. □

In Fig. 3.3, we have plotted the regions $\mathcal{R}(\mathbf{p})$, for p_1 and p_2 ranging from 0 to 1 with a step of 0.01, we also show the boundary of the stability region for the time division multiple access (TDMA) based scheme. From the figure, we can conclude that both systems (TDMA and our proposed system) have the same stability region.

3.3 The Stability Region for the Feedback-Based Random Access Protocol with Energy Harvesting

In this section, we characterize the stability region of the feedback-based random access scheme with energy harvesting, and identify the reduction in the stability region due to energy finiteness. As mentioned before, the queues are interacting, which can be decoupled using

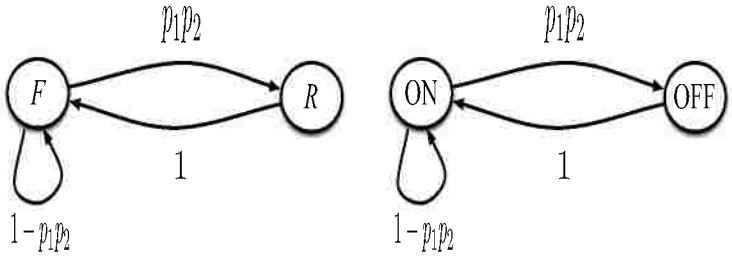

(a) The two-state Markov chain model for B_1

(b) The two-state Markov chain model for B_2

FIGURE 3.4: Batteries Markov chain model.

the dominant system technique. In the dominant system used here ("Dominant System 3"), we assume that every queue always has packets to transmit.

It is worth noting that, a node in this system is assumed to be active if both its packet queue and battery are nonempty at the same time, and idle otherwise. The battery effect is taken into consideration if the energy harvesting rate is less than or equal to the energy consumption rate, and ignored otherwise. So we should first study the conditions under which the effect of the batteries will not be ignored. To figure out those, we should start by calculating the energy consumption rate at both batteries, B_1 and B_2.

In this dominant system, the batteries are assumed to be saturated. This means they always have energy to consume. In this case, the transmission state of B_1 can be represented by the two-state Markov chain shown in Fig. 3.4(a); note that in this case queue B_1 will be either in the Transmission state denoted by F or in the Retransmission state denoted by R in Fig. 3.4(a). Fig. 3.4(b) shows the Markov chain model for B_2, which has two states denoted by ON when B_1 is in the F state and OFF when B_1 is the R state (when Q_1 is in the R state Q_2 will be in the back off, OFF state). It is straightforward to show that the steady state distributions for the two Markov chains shown in Fig. 3.4 are given by

$$\pi_F = \pi_{\text{ON}} = \frac{1}{1+p_1p_2}, \quad \pi_R = \pi_{\text{OFF}} = \frac{p_1p_2}{1+p_1p_2}. \tag{3.6}$$

The energy consumption rate $\mu_1^{''}$ of B_1 is given by

$$\mu_1^{''} = p_1\pi_F + \pi_R = \frac{p_1(1+p_2)}{1+p_1p_2}. \tag{3.7}$$

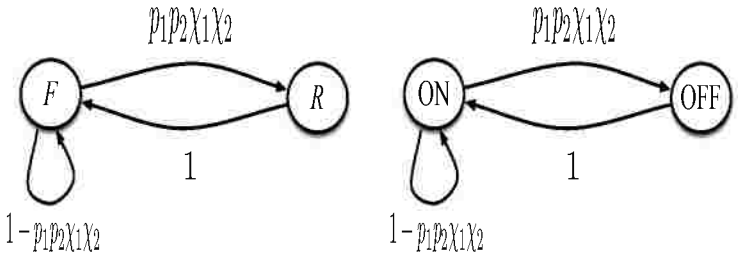

(a) The two-state Markov chain model for Q_1

(b) The two-state Markov chain model for Q_2

FIGURE 3.5: packet queues Markov chain model.

The energy consumption rate $\mu_2^{''}$ of B_2 is

$$\mu_2^{''} = p_2\pi_{ON} = \frac{p_2}{1+p_1p_2}. \tag{3.8}$$

So the conditions under which the batteries affect the system are stated in the following lemma.

Lemma 3.5. *For a given access probabilities, p_1 and p_2, the finiteness of energy causes losses in the stability region if*

$$\delta_1 \leq \frac{p_1(1+p_2)}{1+p_1p_2}, \quad \delta_2 \leq \frac{p_2}{1+p_1p_2}. \tag{3.9}$$

Then we calculate the fractions of time when B_1 and B_2 are being active which follow from Littles theorem. The fractions of time B_1 and B_2 are active, χ_1 and χ_2, are given by

$$\chi_1 = \frac{\delta_1(1+p_1p_2)}{p_1(1+p_2)}, \quad \chi_2 = \frac{\delta_2(1+p_1p_2)}{p_2}. \tag{3.10}$$

In the sequel, we analyze three different systems: system A, system B, and system C. In system A, Q_2 has energy constraint while Q_1 does not. In system B, Q_1 has energy constraint while Q_2 does not. In system C, both Q_1 and Q_2 have energy constraints. For each system, we derive the stability condition for each queue and get the boundary of the stability region.

3.3.1 System A

In this system, we have two different cases. If $\delta_2 > \frac{p_2}{1+p_1p_2}$, the role of B_2 is ruled out as the energy arrival rate is greater than the energy consumption rate and the energy queue will saturate. The steady state distribution of the two state Markov chains shown in Fig. 3.5 for Dominant System 3 with $\chi_1 = \chi_2 = 1$ can be easily derived. This leads to the following stability condition.

$$\lambda_1 < \frac{p_1}{1+p_1p_2}, \quad \lambda_2 < \frac{p_2}{1+p_1p_2}. \tag{3.11}$$

For the other case with $\delta_2 \leq \frac{p_2}{1+p_1p_2}$, the energy queue B_2 will affect the stability condition. By a parallel argument, we can find the stability condition to be given as follows.

$$\lambda_1 < \frac{p_1}{1+p_1p_2\chi_2}, \quad \lambda_2 < \frac{p_2\chi_2}{1+p_1p_2\chi_2}. \tag{3.12}$$

The stability region of system A can be found as the union over $0 \leq p_1 \leq 1$ and $0 \leq p_2 \leq 1$ of the stability regions given in (3.11) with $\delta_2 > \frac{p_2}{1+p_1p_2}$, and in (3.12) with $\delta_2 \leq \frac{p_2}{1+p_1p_2}$.

The boundary of the stability region for system A can be proved to be given as (proof is omitted due to space limitation)

$$\lambda_1 + \lambda_2 = 1 \quad \text{and} \quad \lambda_2 \leq \delta_2. \tag{3.13}$$

In Fig. 3.6, the regions derived for the dominant system for system A are plotted in green. p_1 and p_2 range from 0 to 1 with a step of 0.01 and $\delta_2 = 0.8$. We also plotted the boundary of the stability region the system without energy constraint. From the figure, we can conclude that due to the energy constraint, there is a loss in the stability region recognized by the white space between the stability boundaries of the systems. This loss occurred as Q_2 cannot be served at a rate greater than the energy harvesting rate. This means, if Q_2 only gains access to channel, its throughput cannot exceed its energy harvesting rate. This illustrates why the stability region of the system with energy constraint cuts the λ_2 axis at $\lambda_2 = \delta_2$.

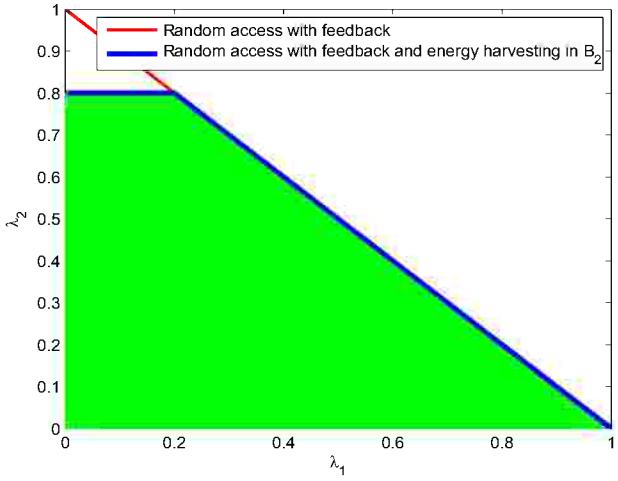

FIGURE 3.6: The stability regions for Random Access with Feedback, and Random Access with Feedback and Energy harvesting in B_2 for $\delta_2 = 0.8$.

3.3.2 System B

In this system, we have two different cases. If $\delta_1 > \frac{p_1(1+p_2)}{1+p_1p_2}$, the role of B_1 is ruled out. The stability condition in this case is as stated above in (3.11).

In the case where $\delta_1 \leq \frac{p_1(1+p_2)}{1+p_1p_2}$, the effect of B_1 is taken into consideration. Following a similar approach to that applied to system A, the stability condition in this case can be written as

$$\lambda_1 < \frac{p_1\chi_1 - p_1p_2\chi_1(1-\chi_1)}{1+p_1p_2\chi_1}, \quad \lambda_2 < \frac{p_2 - p_1p_2\chi_1(1-\chi_1)}{1+p_1p_2\chi_1}. \tag{3.14}$$

To find the boundary of the stability region, we find the union over $0 \leq p_1 \leq 1$ and $0 \leq p_2 \leq 1$ of the stability regions given in (3.11) and in (3.14). For the region defined in (3.14), we should either maximize λ_1 for a given λ_2 or maximize λ_2 for a given λ_1. We consider maximizing $\lambda_2 = \frac{p_2 - p_1p_2\chi_1(1-\chi_1)}{1+p_1p_2\chi_1}$ under the condition $\lambda_1 \leq \frac{p_1\chi_1 - p_1p_2\chi_1(1-\chi_1)}{1+p_1p_2\chi_1}$. It can be easily proved that λ_2 is monotonic decreasing in p_1 and monotonic increasing in p_2. Based on this observation, and using standard optimization analysis, it can be proved that the boundary of the stability region for $\frac{\delta_1}{2} \leq \lambda_1 \leq \delta_1$ is spanned by

$$p_2^* = \frac{\delta_1}{\lambda_1} - 1, \quad p_1^* = \frac{\lambda_1}{\lambda_1 - \delta_1 + 1}. \tag{3.15}$$

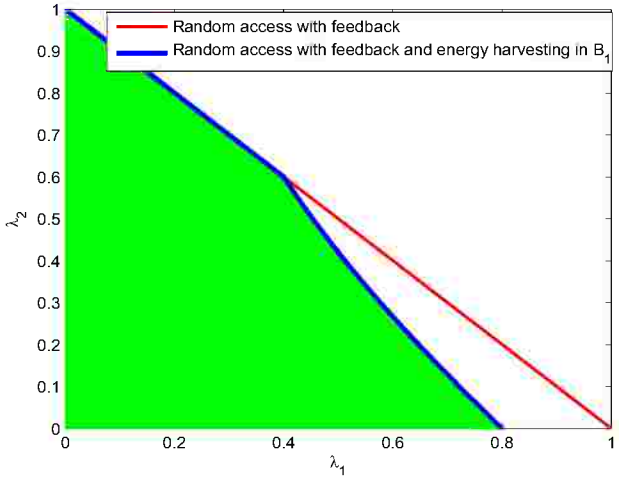

FIGURE 3.7: The stability regions for Random Access with Feedback, and Random Access with Feedback and Energy harvesting in B_1 for $\delta_1 = 0.8$.

From the last equation, it can be easily proved that the boundary of the stability region for $\frac{\delta_1}{2} \leq \lambda_1 \leq \delta_1$ is given by

$$\lambda_2 = \frac{(\delta_1 - \lambda_1)(\lambda_1 - \delta_1 + 1)}{\lambda_1} \quad \text{for} \quad \frac{\delta_1}{2} \leq \lambda_1 \leq \delta_1. \tag{3.16}$$

For $0 \leq \lambda_1 \leq \frac{\delta_1}{2}$, the boundary of the stability region is $\lambda_2 = 1 - \lambda_1$ and is spanned by $p_1^* = 1$ and $0 \leq p_2 \leq 1$. Note that in this region, the boundary of the stability region is not affected by the energy constraint since if $\lambda_1 < \frac{\delta_1}{2}$, B_1 will always be saturated which can be explained as follows. If we consider the extreme case in which the transmission from Q_1 always results in a collision, then every data packet from Q_1 will need two energy packets (one for the initial transmission and one for the retranmission) and if $\lambda_1 \leq \frac{\delta_1}{2}$, then the δ_1 energy arrival rate can always guarantee that B_1 will never be drained out of energy.

The boundary of stability region of the whole system can be characterized as follows.

$$\lambda_2 = \begin{cases} 1 - \lambda_1 & 0 \leq \lambda_1 \leq \frac{\delta_1}{2}. \\ \frac{(\delta_1 - \lambda_1)(\lambda_1 - \delta_1 + 1)}{\lambda_1} & \frac{\delta_1}{2} \leq \lambda_1 \leq \delta_1 \end{cases} \tag{3.17}$$

In Fig. 3.7, the regions derived from the dominant system for system B are plotted in green. p_1 and p_2 range from 0 to 1 with a step of 0.01 and $\delta_2 = 0.8$. From the figure, we can conclude, that due to the energy constraint, there is a loss in the stability region recognized by the white space between the boundaries of both systems. This loss occurred as Q_1 will

not be served at a rate greater than its energy harvesting rate. This means, if Q_1 only gains access to channel, its throughput cannot exceed its energy harvesting rate. Moreover, we can see that the stability region loss due to energy constraint in system B is more than the loss in system A. This can be readily explained since in system B, the queue with the energy constraint is the one used in retransmissions, hence some collision-free retranmission slots can be lost due to energy depletion at the retransmitting node, which is not the case in system A.

3.3.3 System C

In this system, we have four different cases depending on comparing δ_1 and δ_2 to $\frac{p_2}{1+p_1p_2}$ and $\frac{p_1(1+p_2)}{1+p_1p_2}$, respectively.

In the first case, $\delta_1 > \frac{p_1(1+p_2)}{1+p_1p_2}$ and $\delta_2 > \frac{p_2}{1+p_1p_2}$, the role of both batteries is ruled out. The stability condition in this case is as stated before in (3.11).

In the second case, $\delta_1 > \frac{p_1(1+p_2)}{1+p_1p_2}$ and $\delta_2 \leq \frac{p_2}{1+p_1p_2}$, we can rule out B_1 as the arrival rate of energy units is greater than the energy consumption rate of this queue. The stability condition in this case is as stated before in (3.12).

In the third case, $\delta_1 \leq \frac{p_1(1+p_2)}{1+p_1p_2}$ and $\delta_2 > \frac{p_2}{1+p_1p_2}$, the role of B_2 is ruled out and the stability condition in this case is as stated before in (3.14).

In the fourth case in which $\delta_1 \leq \frac{p_1(1+p_2)}{1+p_1p_2}$ and $\delta_2 \leq \frac{p_2}{1+p_1p_2}$, the effect of both batteries is taken into consideration. In this case, the transmission state of Q_1 and Q_2 can be represented by the two-state Markov chain model shown in Fig. 3.5(a) and Fig. 3.5(b), respectively. It is straightforward to show that the steady state distributions for the two Markov chains shown in Fig. 3.5 are given by

$$\pi_F = \pi_{\text{ON}} = \frac{1}{1+p_1p_2\chi_1\chi_2}, \quad \pi_R = \pi_{\text{OFF}} = \frac{p_1p_2\chi_1\chi_2}{1+p_1p_2\chi_1\chi_2}. \tag{3.18}$$

The service rate for Q_1 in Dominant System 3, is given by

$$\begin{aligned} \mu_1 &= (p_1(1-p_2)\chi_1\chi_2 + p_1(1-\chi_2)\chi_1)\pi_F + \chi_1\pi_R \\ &= \frac{p_1\chi_1 - p_1p_2\chi_1\chi_2(1-\chi_1)}{1+p_1p_2\chi_1\chi_2}, \end{aligned} \tag{3.19}$$

where Q_1 is served with probability $p_1(1-p_2)\chi_1\chi_2 + p_1(1-\chi_2)\chi_1$ in the F state. In the R state, Q_1 is served with probability χ_1, which is the probability of having an energy unit in B_1 to support the retransmission.

Similarly, the service rate for Q_2 in this Dominant System, is given by

$$\begin{aligned}\mu_2 &= (p_2(1-p_1)\chi_1\chi_2 + p_2(1-\chi_1)\chi_2)\pi_{ON} + \chi_1\pi_{OFF} \\ &= \frac{p_2\chi_2 - p_1p_2\chi_1\chi_2(1-\chi_1)}{1+p_1p_2\chi_1\chi_2}.\end{aligned} \tag{3.20}$$

Following a similar analysis to what has been presented above, the boundary of stability region of system C can be derived. The stability region boundary depends on the values of δ_1 and δ_2. If $\delta_2 < 1 - \frac{\delta_1}{2}$, the boundary of the stability region is given by

$$\lambda_2 = \begin{cases} \delta_2 & 0 \le \lambda_1 \le \frac{2\delta_1 - \delta_2 + \sqrt{2\delta_2 - 4\delta_1\delta_2 + \delta_2^2 + 1} - 1}{2}. \\ \frac{(\delta_1 - \lambda_1)(\lambda_1 - \delta_1 + 1)}{\lambda_1} & \frac{2\delta_1 - \delta_2 + \sqrt{2\delta_2 - 4\delta_1\delta_2 + \delta_2^2 + 1} - 1}{2} \le \lambda_1 \le \delta_1 \end{cases}, \tag{3.21}$$

and if $\delta_2 \ge 1 - \frac{\delta_1}{2}$, the boundary of the stability region is given by

$$\lambda_2 = \begin{cases} \delta_2 & 0 \le \lambda_1 \le 1 - \delta_2 \\ 1 - \lambda_1 & 1 - \delta_2 \le \lambda_1 \le \frac{\delta_1}{2} \\ \frac{(\delta_1 - \lambda_1)(\lambda_1 - \delta_1 + 1)}{\lambda_1} & \frac{\delta_1}{2} \le \lambda_1 \le \delta_1 \end{cases} \tag{3.22}$$

In Fig. 3.8 and Fig. 3.9, the stability regions derived from the dominant system used for system C are plotted in green for $\delta_1 = \delta_2 = 0.8$ where $\delta_2 \ge 1 - \frac{\delta_1}{2}$ and $\delta_1 = \delta_2 = 0.6$ where $\delta_2 < 1 - \frac{\delta_1}{2}$, respectively. p_1 and p_2 range from 0 to 1 with a step of 0.01 in both figures. From the figures, we can conclude that due to the energy constraint, there is a loss in the stability region recognized by the white space between the boundaries of both systems. Note that if one queue only gains access to channel, its throughput cannot exceed its energy harvesting rate. This explains why the stability region of the system with energy constraint cuts the λ_1 and λ_2 axes at δ_1 and δ_2, respectively.

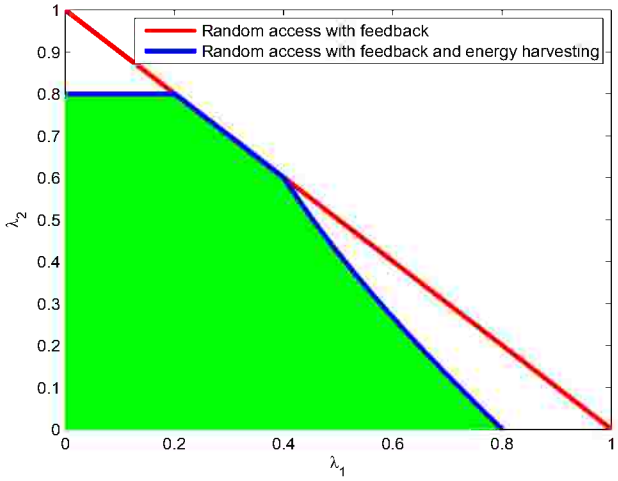

FIGURE 3.8: The stability regions for Random Access with Feedback, and Random Access with Feedback and Energy harvesting in both batteries for $\delta_1 = \delta_2 = 0.8$.

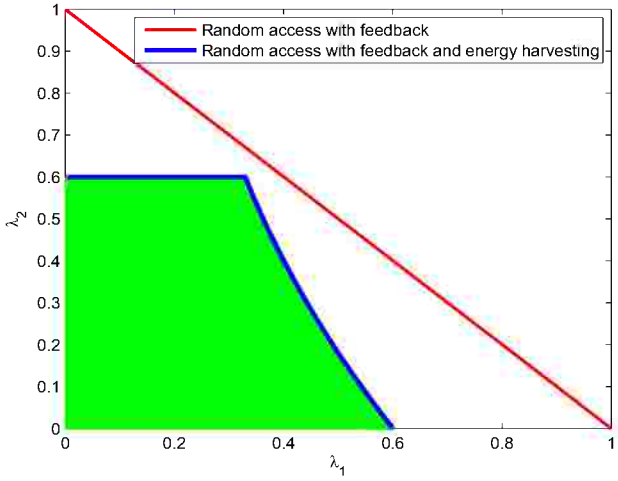

FIGURE 3.9: The stability regions for Random Access with Feedback, and Random Access with Feedback and Energy harvesting in both batteries for $\delta_1 = \delta_2 = 0.6$.